Temperature Dependence of Oxygen Diffusion Into Polymer/Carbon Nanotube Composite Films

Önder Yargı,[1] **Şaziye Ugur,**[1] **Önder Pekcan**[2]
[1] *Department of Physics, Istanbul Technical University, Maslak 34469, Istanbul, Turkey*

[2] *Faculty of Arts and Science, Kadir Has University, Cibali 34320, Istanbul, Turkey*

This study examines the transport properties of polystyrene (PS)/multiwalled carbon nanotube (MWNT) composite films taking into consideration both MWNT composition and temperature, via fluorescence technique. Three different (3, 15, and 40 wt%) MWNT content films were prepared from PS/MWNT mixtures by annealing them at 170°C, above the glass transition temperature of PS for 10 min. The diffusivity of the PS/MWNT composite was determined by performing oxygen (O_2) diffusion measurements within a temperature range of 24 to 70°C for each film and pyrene (P) was used as the fluorescent probe. The diffusion coefficients (*D*) of oxygen were determined by the fluorescence quenching method assuming Fickian transport. Results indicated that *D* values are strongly dependent on both temperature and the MWNT content in the film and it was also observed that *D* coefficients obey Arrhenius behavior, from which diffusion energies were produced and increased along with increases of MWNT content. POLYM. ENG. SCI., 52:172–179, 2012. © 2011 Society of Plastics Engineers

INTRODUCTION

There has been growing interest in producing new materials by filling polymers with inorganic natural (minerals) and/or synthetic (carbon black and silica) compounds [1–5] because single component polymer films have poor mechanical and gas barrier properties. Composite polymers display improved mechanical and gas barrier properties and a decrease in flammability in comparison with simple polymers [6]. The enhancement in barrier properties in composites depends on several factors, such as the amount, length, and width of the filler, as well as the orientation and dispersion of the filler particles. For more than 50 years, polymer scientists have been interested in the influence of fillers on gas diffusion through polymer membranes [7–11], and this study expands on that research by bringing to light the effects of mineral fillers on the performance of oxygen sensors. Gorrasi et al. [8] studied the transport properties of *n*-pentane and dichloromethane vapors in polypropylene-organophilic layered silicate nanocomposites with different clay concentrations, and it was found that the permeability of both solvent vapors was reduced, mainly as a result of the decreased diffusion, since the solubility was less affected by the presence of fillers. Lu et al. [9] examined the influence of 10 nm diameter silica particles on oxygen diffusion in polydimethylsiloxane (PDMS) polymer film. A decrease was observed in oxygen diffusion coefficients, *D*, with increases of silica content. This reduction in *D* was attributed to the tortuous path for diffusing gas molecules and the reduced molecular mobility of polymer chains caused by the filler particles.

Carbon nanotubes (CNT) have been identified as fundamentally new nanoporous materials that show great potential for sensors [12, 13], composites [14], catalytic supports [15], and as membrane materials [16, 17]. Significant effort has been devoted to the fabrication of mixed matrix membranes by using carbon nanotubes as filler with great potential [18]. Many researchers have studied composites composed of conductive materials/polymers as candidates for chemical vapor sensors because composite materials have the advantages of high sensitivity and reproducibility, good processability, and reasonable costs [19]. Polymer/conductive material composites used as sensors have the following properties: (1) numerous possibilities for preparation of various types with a wide range of selectivity owing to the diversity of the chemical and physical properties of polymers, (2) sensitive, rapid, and reversible responses to analytes, and (3) the most interesting materials can transform a chemical signal into an electric signal [19]. The polymer/conducting material composites are prepared by blending polymer matrices with carbon black, metal powder, carbon fiber, graphite, or carbon nanotubes. These composites as chemical vapor sensors are expected to be utilized for a broad spectrum of applications in the detection of environmental gases, solvent leaks, and identification of polymers, in addition

Correspondence to: Şaziye Ugur; e-mail: saziye@itu.edu.tr
DOI 10.1002/pen.22061
Published online in Wiley Online Library (wileyonlinelibrary.com).

to other uses as well [20]. Among the various conductive materials, carbon nanotubes (CNT) have attracted notable attention because of their unique structure and remarkable physical properties. These properties make them a strong candidate for active materials in electronics, field emission devices, and chemical vapor sensors. The chemical vapor sensing property of CNT is due to the fact that CNT is a nanosized material and has a high aspect ratio, resulting in high sensitivity and rapid chemical vapor adsorption [21].

In early 2000, the potential for CNTs as gas sensors was first reported in a study that noted an increase in conductivity by several orders of magnitude upon exposure of CNTs to oxygen [22]. There are two basic types of CNTs: single-wall carbon nanotubes (SWNT) and multiwall carbon nanotubes (MWNT) [23]. In this respect, more researchers have devoted effort to the fabrication of mixed matrix membranes by dispersing either single-walled or multiwalled carbon nanotubes into various polymer matrices. The properties of polymer nanocomposites containing carbon nanotubes depend on several factors, in addition to the polymer: the synthetic process used to produce nanotubes; the nanotube purification process; the amount and types of impurities in the nanotubes; diameter, length, and aspect ratio of the nanotube's objects in the composite (isolated, ropes, and/or bundles); and the orientation of the nanotubes in the polymer matrix. Kim et al. [24] studied how incorporating CNTs into the polyimidesiloxane matrix impacted gas separation performance. They observed that the addition of small CNTs to the copolymer matrix reduced the permeability of helium reduced and hindered the diffusion of nitrogen as a result of the impermeable properties of CNTs.

Oxygen is considered to be one of the most important reactants in the diffusion phenomenon. The control of the diffusion of oxygen is of particular importance in polymer oxidative degradation, protective coatings, and in the design of polymeric membranes for separation processes in the production of films for the packing industry, as well as in the development of biocompatible materials [25]. Oxygen diffusivity in polymers is most commonly determined by measuring the rate of oxygen permeation across a membrane by exposing one side of the polymer film to oxygen at time zero and measuring the flux of oxygen across the film as a function of time. Knowing the dimensions of the film and the partial pressure of oxygen on the high-pressure side, allows for a calculation of the diffusion coefficient from the flux [26]. The diffusion coefficient of oxygen is determined from the kinetics of the approach of the O_2 flux to its steady-state. Because oxygen is such a powerful quencher of fluorescence and phosphorescence, this property is useful for determining such values. Another approach, developed by Cox and Dunn, also looks at large samples [27] utilizing a square cell measuring 1 cm height. The cell is filled with a polymer containing the dye and all oxygen is removed. Cox and Dunn irradiated a thin (1 mm) middle cross-section of the cell, and then allowed oxygen to diffuse into the cell from the top. As the oxygen concentration profile propagates through the illuminated middle slice, the emission intensity is quenched.

Several spectroscopic techniques that utilize oxygen quenching to determine the rate of oxygen diffusion through polymer films have been reported. Cox [28] and Dunn [29], and MacCallum and Rudkin [30] measured oxygen diffusion coefficients by fluorescence quenching in planar sheets of poly(dimethyl siloxane) [28], filled poly(dimethyl siloxane) samples [29], and polystyrene [30]. They monitored oxygen quenching of a fluorophore as a function of time by assuming that fluorophores dispersed homogeneously within the film. The mathematical determination of D varied, but a single underlying assumption in all cases was that the time-dependent emission intensity was measured during the experiment. In some cases, the intensity versus time curve was converted to a concentration versus time curve using the Stern-Volmer relationship [28, 29]. Lu et al. [31–33] have used time-scan experiments to measure the decay of luminescence intensity as oxygen diffuses into polymer films under constant illumination and the growth of intensity as oxygen diffuses out of the film. They interpreted their data with the aid of theoretical expressions based on Stern-Volmer quenching kinetics with Fick's laws of diffusion. In some of our earlier studies, we examined the effect of temperature [34] and Na-activated bentonite (MNaLB) clay content [35] on the oxygen diffusion coefficient, D, in PS/MNaLB composite films by using a steady state fluorescence (SSF) technique. In these studies, we found that D values increased by increasing the temperature [34] and MNaLB content [35].

In the present study, the feasibility of MWNT doped P labeled PS composite films (PS/MWNT) for possible oxygen gas sensing applications was investigated. The gas sensitivity of composite films was evaluated by measuring the change in P fluorescence intensity in the presence of oxygen for different MWNT contents at various temperatures. For this purpose, three different sets of composite films were prepared from PS latex-MWNT mixtures with 3, 15, and 40 wt% MWNT content by annealing at 170°C for 10 min. A steady-state fluorescence technique (SSF) was used to study oxygen diffusion into these films over the temperature range of 24 to 70°C. The time drive mode of the SSF spectrometer was employed to monitor the intensity change of excited P during oxygen penetration into composite films and a model was developed by combining Stern-Volmer and Fickian models for low quenching efficiency to measure the oxygen diffusion coefficient, D.

EXPERIMENT

Materials

PS particles were produced via a free emulsion polymerization process. The polymerization was performed

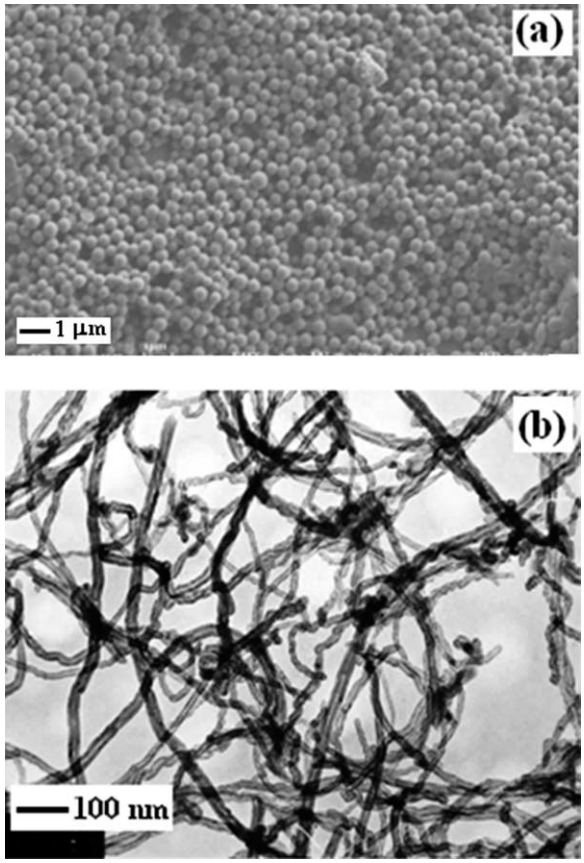

FIG. 1. (a) SEM picture of pure PS latex. (b) SEM picture of MWNT.

batch-wisely using a thermostatted reactor equipped with a condenser, thermocouple, mechanical stirring paddle, and nitrogen inlet. The agitation rate was 400 rpm and the polymerization temperature was controlled at 70°C. Water (100 ml) and styrene (5 g) were first mixed in the polymerization reactor where the temperature was kept constant (at 70°C). The potassium peroxodisulfate (KPS) initiator (0.1 g) dissolved in a small amount of water (2 ml), was then introduced to induce styrene polymerization. The polymerization was conducted over a period of 18 h. The polymer had a high glass transition temperature ($T_g = 105$°C) and the latex dispersion has an average particle size of 400 nm. Figure 1a shows the SEM image of the PS latex produced for this study.

Commercially available MWNTs (Cheap Tubes Inc., VT; 10–30 μm long, average inner diameter 5–10 nm, outer diameter 20–30 nm, density approximately 2.1 g/cm^3, and purity higher than 95 wt%) were used as supplied in black powder form without further purification. A stock solution of MWNTs was prepared following the manufacturers regulations: nanotubes were dispersed in deionized (DI) water with the aid of polyvinyl pyrolidone (PVP) in the proportions of 10 parts MWNTs; 1 to 2 parts PVP and 2.000 parts DI water by bath sonication for 3 h. PVP is a good stabilizing agent for dispersion of carbon nanotubes, enabling preparation of polystyrene composites from dispersions of MWNT in a polystyrene solution. Figure 1b shows the TEM image of MWNTs used in this study (available at: www.cheaptubesinc.com).

Preparation of PS/MWNT Composite Films

A 15 g/l solution of polystyrene (PS) in water was prepared separately. The dispersion of MWNT in water was mixed with the solution of PS yielding the required ratio of MWNT in the PS latex. Three different mixtures were prepared with 3, 15, and 40 wt% MWNT. Each mixture was stirred separately for 1 h followed by sonication for 30 min at room temperature. By placing the same number of drops on a glass plates with similar surface areas (0.8×2.5 cm^2) and allowing the water to evaporate at 60°C in the oven, dry films were obtained. After drying, samples were separately annealed above T_g of PS (170 ± 2°C) for 10 min. Following the annealing process, films were removed from the oven and cooled down to room temperature. Figure 2 shows SEM micrographs of composite films with 15 and 40 wt% MWNT content before and after annealing at 170°C, respectively. After the annealing treatment, SEM images clearly present the coalescence of PS particles in which the PS particle shape has been destroyed and the microstructure of the latex has completely disappeared. The thickness of the films was determined from the weight and the density of samples (≈ 3 μm).

Fluorescence Measurements

In fluorescence measurements for oxygen diffusion experiments, films were placed in a round quartz tube filled with nitrogen, in a Perkin Elmer Model LS-50 fluorescence spectrophotometer. Slit widths were kept at 8 nm. Experiments were carried out at 24, 40, 50, 60, and 70°C temperatures. A thermistor-based digital temperature probe was used to monitor temperatures during the diffusion experiments. The temperature in the chamber was observed to remain constant within ± 2°C during the course of diffusion measurements. In all experiments, P was excited at 345 nm and the intensity at the emission maximum (395 nm) was used for the P intensity (I_p) measurements. I_p was monitored against time at different temperatures for each MWNT content composite film after the quartz tube was opened to the air for O_2 diffusion experiments by using a time-drive mode of spectrophotometer. Since the diffusion measurements required that oxygen permeate only from one surface of the film, to further ensure that lateral diffusion did not affect results, a small region in the center of the films was masked off for measurement using black tape on the opposite side of the window from the samples.

THEORETICAL CONSIDERATIONS

Fluorescence Quenching by Oxygen

The mechanism of oxygen quenching involves a sequence of spin allowed internal conversion processes

 DOI 10.1002/pen

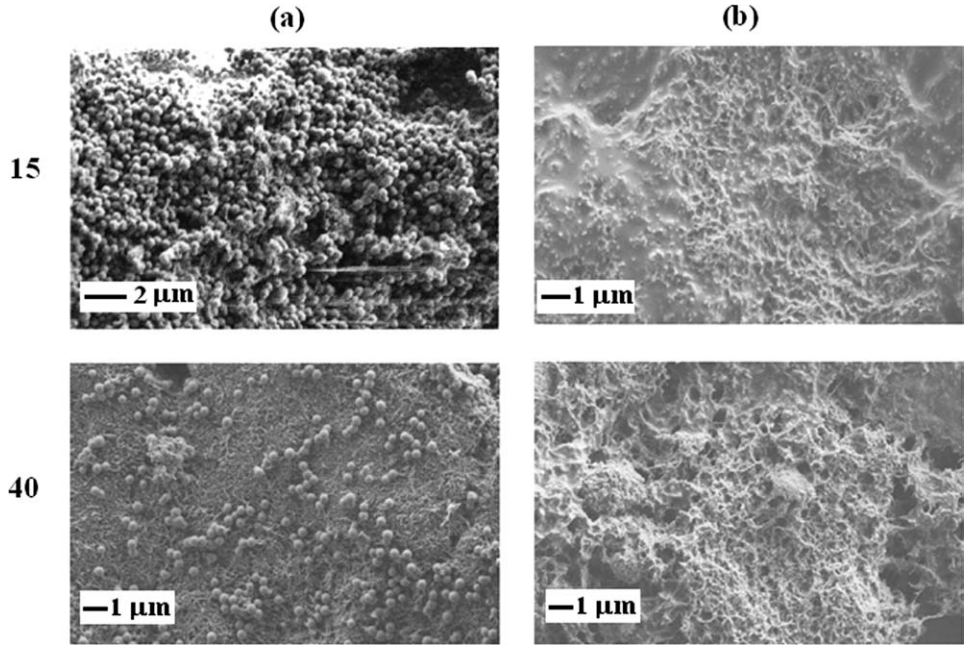

FIG. 2. Scanning electron micrographs (SEM) of composite films prepared with 15 and 40 wt% MWNT content a) before and b) after annealing at 170°C temperature.

which take place within a weakly associated encounter complex between the probe and oxygen. The product is either a singlet ground state or an excited triplet species [36]. Data generated from oxygen quenching studies on fluorescence molecules in homogeneous medium are usually analyzed using the Stern-Volmer relation (*Eq. 1*), provided that the oxygen concentration $[O_2]$ is not too high [37].

$$\frac{I_0}{I} = 1 + k_q \tau_0 [O_2]. \quad (1)$$

where I and I_0 are, respectively, the fluorescence intensities in the presence and absence of oxygen, k_q is the bimolecular quenching rate constant and τ_0 is the fluorescence lifetime in the absence of O_2. This equation requires that the decay of fluorescence is single exponential and, moreover, that quenching interactions occur with a unique rate constant, k_q. From the slope of a plot of I_0/I versus $[O_2]$, k_q can be determined provided that τ_0 is known.

Diffusion in Plane Sheet

Fick's second law of diffusion was used to model diffusion phenomena in plane sheet. The following equation is obtained by assuming a constant diffusion coefficient, for concentration changes in time [38]

$$\frac{C}{C_0} = \frac{x}{d} + \frac{2}{\pi} \sum_{n=1}^{\infty} \frac{\cos n\pi}{n} \sin \frac{n\pi x}{d} \exp\left(-\frac{Dn^2\pi^2 t}{d^2}\right), \quad (2)$$

where d is the thickness of the slab, D is the diffusion coefficient of the diffusant, and C_0 and C are the concentration of the diffusant at time zero and t, respectively. x corresponds to the distance at which C is measured. We can replace the concentration terms directly with the amount of diffusant, M, by using the following relation:

$$M = \int_v C dV. \quad (3)$$

When *Eq. 3* is considered for a volume element in the plane sheet and substituted in *Eq. 2*, the following solution is obtained [38]:

$$\frac{M_t}{M_\infty} = 1 - \frac{8}{\pi^2} \sum_{n=0}^{\infty} \frac{1}{(2n+1)^2} \exp\left(-\frac{D(2n+1)^2\pi^2 t}{d^2}\right). \quad (4)$$

Here M_t and M_∞ represent the amounts of diffusant entering the plane sheet at time t and infinity, respectively.

RESULTS AND DISCUSSIONS

Diffusion Coefficients

Normalized pyrene intensity, I_p, curves are presented in Fig. 3 as a function of time for the 40 wt% MWNT content film exposed to oxygen at three different temperatures. It is seen that as oxygen diffused through the planar film, the emission intensity of the pyrene decreased according to *Eq. 1* for each temperature. The rate of decrease in intensity is higher at higher temperatures predicting the more rapid quenching of excited pyrene molecules by O_2 molecules diffused into the films. All

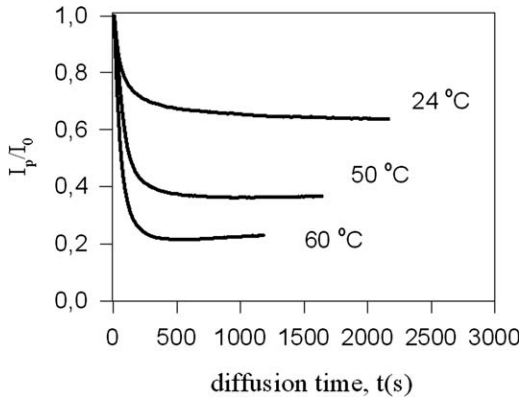

FIG. 3. The time behavior of the pyrene, P, and fluorescence intensity, *I*, during oxygen diffusion into the 40 wt% MWNT content film at various temperatures. Numbers on each curves indicate the temperature.

curves behave almost in the same fashion, as oxygen diffused through and equilibrated in the film. It is also seen that the diffusion curves reach their equilibrium value at shorter times for higher temperatures. In order to interpret the above findings, *Eq. 1* can be used by expanding in a series for low quenching efficiency, i. e. $k_q\tau_0[O_2] \ll 1$ which then produces the following useful result:

$$I \approx I_0\left(1 - k_q\tau_0[O_2]\right). \tag{5}$$

During diffusion into the films, P molecules are quenched in the volume which is occupied by O_2 molecules at time, *t*. Then P intensity at time *t* can be represented by the volume integration of *Eq. 5* as

$$I_p = \frac{\int Idv}{\int dv} = I_0 - \frac{k_q\tau_0 I_0}{V}\int dv[O_2], \tag{6}$$

where *dv* is the differential volume and *V* is the total volume of the film as shown in Fig. 4. In Fig. 4, oxygen diffusion into the film is presented at different time steps, where pyrene quenching take place at $t > 0$ and levels off at $t = \infty$. Performing the integration the following relation is obtained

$$I_p = I_0\left(1 - k_q\frac{\tau_0}{V}O_2(t)\right), \tag{7}$$

where $O_2(t) = \int dv[O_2]$ is the amount of oxygen molecules diffused into the film at time *t*. If it is assumed that $O_2(t)$ corresponds to M_t then *Eq. 4* can be combined for oxygen with *Eq. 7* and the following useful relation is obtained which can be used to interpret the diffusion curves in Fig. 3

$$\frac{I_p}{I_0} = A + \frac{8C}{\pi^2}\exp\left(-\frac{D\pi^2 t}{d^2}\right), \tag{8}$$

where *d* is now present as the film thickness, *D* is the oxygen diffusion coefficient, $C = \frac{k_q\tau_0 O_2(\infty)}{V}$ and $A = 1 - C$. Here $O_2(\propto)$ is the amount of oxygen molecules diffused into the film at time infinity. The logarithmic form of *Eq. 8* can be written as follows:

$$\mathrm{Ln}\left(\frac{I_p}{I_0} - A\right) = \mathrm{Ln}\left(\frac{8C}{\pi^2}\right) - \frac{D\pi^2}{d^2}t \tag{9}$$

Figure 5 presents a logarithmic plot of the data in Fig. 3 ($Ln(I_p/I_0 - A)$) versus diffusion time for the 40 wt% MWNT content film at three different temperatures. *Eq. 9* is fitted to these data by the linear least square method, and the oxygen diffusion coefficients, *D*, at different temperatures were produced from the slopes of the plots. Similar fittings were done for the other MWNT content films and *D* values were obtained for different temperatures and collected in Table 1. The average *D* values were determined from three or five measurements on different samples in each case and the standard deviations on *D* values are also given in Table 1. *D* values versus temperature are plotted for three MWNT content films in Fig. 6a. It is seen that *D* coefficients are strongly dependent on both temperature and MWNT content in the film. It is worthy to note that, as expected, *D* increases with increases in temperature for all composite films. The increasing of *D* values for the three films is seen clearly especially above a certain temperature (50°C). Increases in temperature naturally increase the Brownian motion of oxygen molecules giving them more chance to meet the P molecules in the composite film.

On the other hand, increasing the MWNT content also increases the *D* values. As seen in Fig. 1, the structure of PS particles is spherical, while MWNT is long and cylindrical in structure. This difference in the formation of defects or voids in the films enhances the diffusion rate of oxygen along the film by increasing the surface area against the oxygen molecules. This result is consistent with microstructural analysis. SEM micrographs of com-

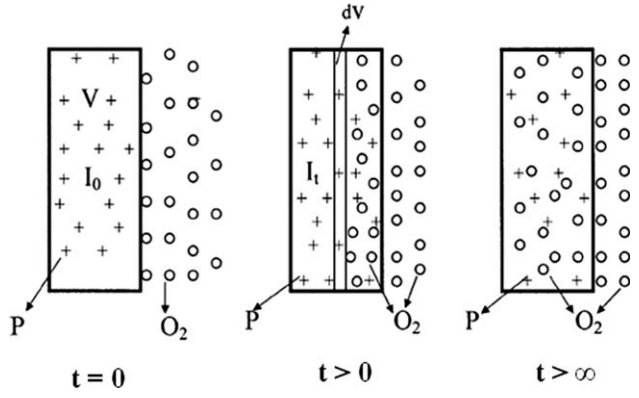

FIG. 4. Cartoon representation of oxygen diffusion into the film at elevated time intervals.

DOI 10.1002/pen

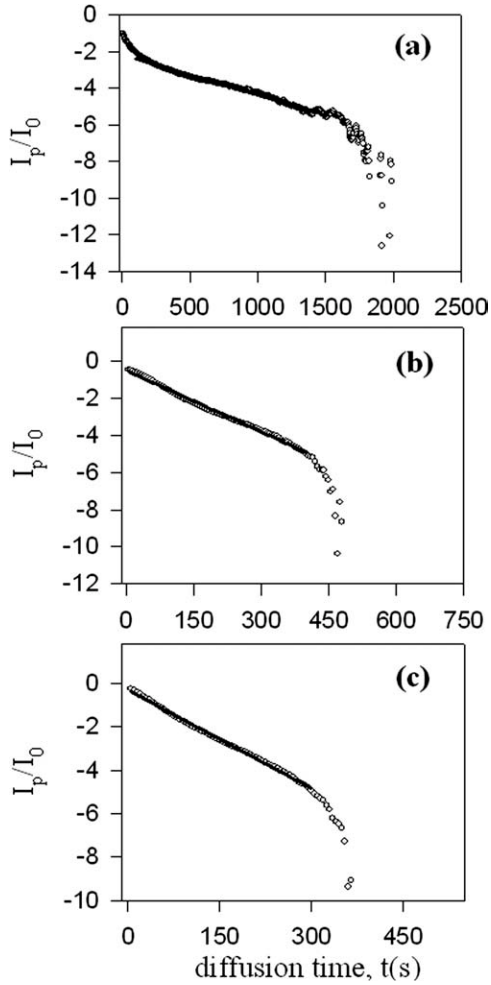

FIG. 5. Logarithmic plot of the data in Fig. 3 according to *Eq. 9* in the text. The slopes of the curves produced diffusion coefficients, *D*. Numbers on each curve indicate the temperature.

posite films with 15 and 40 wt% MWNT content in Fig. 2 also confirm this picture. Before annealing, no deformation in PS particles is observed and PS particles keep their original spherical shapes. After annealing treatment at 170°C, SEM images show that complete particle coalescence has been achieved. It can be clearly seen that the composite film consists of a network of bundles, especially in the 40 wt% MWNT content film, and indicates significant porosity. As shown in Fig. 2, carbon nanotubes are not well distributed in the polymer matrix and voids between the carbon nanoparticles and polymer matrix appeared allowing oxygen molecules to move rapidly. Therefore, O_2 molecules can easily pass through these voids. Thus, the permeability of O_2 gas is increased, yielding high diffusion coefficients. As a result, more rapid diffusion of oxygen [35] into the three composite films occurs due to the presence of a large number of microvoids in these films.

These results are consistent with previous studies [39–42]. Generally, enhancement in the gas permeability of polymers by putting inorganic fillers into the organic polymer resulted from the disturbed polymer chain packing by the nanofillers [39]. Therefore, the well dispersed state of carbon nanotubes and their good adherence effectively increases gas permeability as the result of effective insertions between the polymer chains of the matrix. The addition of 2 wt% of modified carbon nanotubes loading to the polyethersulfone resulted in about 19.97% increases in the permeability of CO_2, while the permeability of CH_4 increased up to 33.79%. However, for small gas molecules, such as CO_2, the permeability increased slightly with the addition of carbon nanotubes in the polyethersulfone (PES) host matrix. The main pathways of gas transport through the mixed matrix membranes are through the dense layer of the PES matrix, highly selective carbon nanotubes and nonselective gaps or voids between the matrix and sieve particles. It was observed

TABLE 1. Experimentally produced *D* values.

	$D \times 10^{-11}(\text{cm}^2 \cdot \text{s}^{-1})$		
T (°C)	3	15	40
24	1 ± 0.04	2 ± 0.2	4 ± 0.3
40	6 ± 0.1	4 ± 0.4	5 ± 0.9
50	8 ± 0.5	12 ± 0.2	19 ± 0.1
60	10 ± 1	15 ± 0.8	25 ± 0.6
70	17 ± 2	28 ± 0.8	31 ± 3

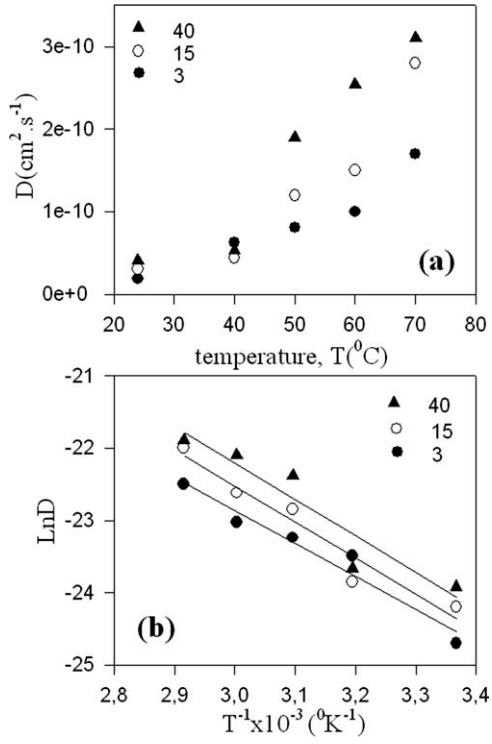

FIG. 6. (a) Plot of the diffusion coefficients, *D,* versus temperatures, *T* for the 3, 15, and 40 wt% MWNT content films. (b) Plot of the logarithmic form of *Eq. 10* for the data in Table 1. ΔE_D values are obtained from the slopes of the straight lines for each MWNT content film, respectively.

TABLE 2. Experimentally produced diffusion energies.

MWNT (wt%)	3	15	40
ΔE_D (kJ mol^{-1})	68	76	100

that the main factor affecting the increase of CH_4 permeability with the addition of carbon nanotubes into the polymer host resulted from the extremely rapid diffusion of gas molecules adsorbed inside the carbon nanotubes. FESEM data also showed that the carbon nanotubes are well dispersed in the polymer matrix and serve as channels to transport gas molecules [40–42]. It is known that the addition of filler into polymer films above a critical percentage creates voids [43, 44] in the polymer matrix. Ponomarev and Gouterman [43] have reported that the addition of high amounts of titanium oxide (TiO_2) in pressure sensitive (PSP) paints cause the presence of a large fraction of microvoids inside the films. As a result, air can diffuse very rapidly to the inside of the coating through these voids.

Diffusion Energies

The diffusion of small molecules through membranes can be described as a thermally activated process that obeys Arrhenius behavior. The temperature dependence of the diffusion coefficient, D, can be written as follows:

$$D = D_0 \exp\left(\frac{-\Delta E_D}{k_B T}\right). \quad (10)$$

Here k_B is the Boltzmann constant, D_0 is pre-exponential factor and ΔE_D is the energy as associated with the oxygen diffusion. The activation energy was determined from the logarithmic plots of the D coefficient against the reciprocal of the absolute temperature. In Fig. 6b, Ln(D) was plotted versus 1000/T for the different clay fraction, respectively. The value of the activation energy associated with oxygen diffusion (ΔE_D) for different MWNT fractions was calculated from the slope of these plots by fitting the data in Fig. 6b to the *Eq. 10* by a least square fit. The results are given in Table 2, where ΔE_D increases with increasing MWNT content. The energy need for oxygen diffusion in the high MWNT medium is much higher than in a low MWNT environment. Most probably, the motion of O_2 molecules is screened by the large number of MWNT barriers during their journey in the high MWNT content medium, in where O_2 needs higher energy to overcome this difficulty.

CONCLUSION

In this article, we examined the use PS/MWNT nanocomposites as fluorescent oxygen sensors and how oxygen diffusion is affected by both MWNT content and temperature using the fluorescence technique. Fluorescence experiments were carried out on composite films containing pyrene as a sensor dye. We monitored the change in fluorescence intensity as oxygen was allowed to diffuse into the film and the presence of oxygen was detected through measurements of fluorescence quenching. Diffusion experiments demonstrated that the quenching rate during oxygen diffusion was completely consistent with Fickian diffusion. The diffusion coefficients increased drastically with both increases of MWNT content and also of the temperature and this increase was explained via the existence of large amounts of pores in composite films which facilitate oxygen penetration into the structure.

We thus have proposed a simple, rapid, and practical means to measure the diffusion of oxygen into PS/MWNT composite films. This study illustrates that PS/MWNT nanocomposites have useful properties as fluorescent oxygen sensors, and a simple SSF technique can be used to measure the diffusion coefficient of oxygen molecules into these films quite accurately.

REFERENCES

1. R.A. Vara, K.D. Jandt, F.J. Kramer, and F.P. Giannelis, *Chem. Mater.*, **8**, 2628 (1996).
2. M.W. Noh and D.C. Lee, *Polym. Bull.*, **42**, 619 (1999).
3. H.Z. Friedlander and C.R. Grink, *J. Polym. Sci. Part B: Polym. Lett.*, **2**, 475 (1964).
4. C. Kato, K. Kuroda, and H. Takahara, *Clays Clay Miner.*, **29**, 294 (1981).
5. J.G. Doh and I. Cho, *Polym. Bull.*, **41**, 511 (1998).
6. Y. Li, B. Zhao, S.B. Xie, and S. Zhang, *Polym. Int.*, **52**, 892 (2003).
7. R.M. Barrer, in *Diffusion in Polymers*, J. Crank and G.S. Park, Eds., Academic Press, New York, 164 (1968).
8. G. Gorrasi, M. Tortora, V. Vittoria, D. Kaempfer, and R. Mülhaupt, *Polymer*, **44**, 3679 (2003).
9. X. Lu, I. Manners, and M.A. Winnik, *Macromolecules*, **34**, 1917 (2001).
10. R.K. Bharadwaj, *Macromolecules*, **34**, 9189 (2001).
11. P.G. Villaluenga, M. Khayet, M.A. Lopez-Manchado, J.L. Valentin, B. Seoane, and J.I. Mengual, *Eur. Polym. J.*, **43**(4), 1132 (2007).
12. J. Kong, N.R. Franklin, C. Zhou, M.G. Chapline, S. Peng, K. Cho, and H. Dai, *Science*, **28**, 622 (2000).
13. P.G. Collins, K. Bradley, M. Ishigami, and A. Zettl, *Science*, **287**, 1801 (2000).
14. P. Calvert, *Nature*, **399**, 210 (1999).
15. J.M. Planei, N. Coustel, B. Coq, V. Brotons, P.S. Kumbhar, R. Dutartre, P. Geneste, P. Bernier, and P.M. Ajayan, *J. Am. Chem. Soc.*, **116**, 7935 (1999).
16. B.J. Hinds, N. Chopra, T. Rantell, R. Andrews, V. Gavalas, and L.G. Bachas, *Science*, **303**, 62 (2003).
17. J.K. Holt, H.G. Park, Y. Wang, M. Stadermann, A.B. Artyukhin, C.P. Grigoropoulos, A. Noy, and O. Bakajin, *Science*, **312**, 1034 (2006).
18. A.F. Ismail, T.D. Kusworo, and A. Mustafa, *J. Membr. Sci.*, **319**, 306 (2008).

19. X.M. Dong, R.W. Fu, M.Q. Zhang, B. Zhang, and M.Z. Rong, *Carbon*, **42**, 2551 (2004).
20. Y. Luo, Y. Liu, and Q. Yu, *Thin Solid Films*, **515**, 4016 (2007).
21. M.L.Y. Sin, G.C.T. Chow, G.M.K. Wong, and W.J. Li, *IEEE Trans. Nanotechnol*., **6**, 571 (2007).
22. A. Goldoni, R. Larciprete, L. Petaccia, and S. Lizzit, *J. Am. Chem. Soc*., **125**, 11329 (2003).
23. Y. Lin, B. Zhou, K.A. Shiral Fernando, P. Liu, L.F. Allard, and Y.P. Sun, *Macromolecules*, **36**, 7199 (2003).
24. S. Kim, T.W. Pechar, and E. Marand, *Desalination*, **192**, 330 (2006).
25. T. Pietraß, J.L. Dewald, C.F.M. Clewett, D. Tierney, A.V. Ellis, S. Dias, A. Alvarado, L. Sandoval, S. Tai, and S.A. Curran, *J. Nanotechnol*., **6**, 135 (2006).
26. W.Y. Wen, *Chem. Soc. Rev*., **22**, 117 (1993).
27. M.E. Cox and B. Dunn, *J. Polym. Sci. Part A: Polym. Chem*., **24**, 621 (1986).
28. M.E. Cox, *J. Polym. Sci*., **24**, 621 (1986).
29. M.E. Cox and B. Dunn, *J. Polym. Sci*., **24**, 2395 (1986).
30. J.R. MacCallum and A.L. Ruddin, *Eur. Polym. J*., **14**, 655 (1978).
31. X. Lu, I. Manners, and M.A. Winnik, in *Fluorescence Spectroscopy; New Trends in Fluorescence Spectroscopy*, B. Valuer and J.C. Brochan, Eds., Springer Verlag, New York, Chapter 12, 229 (2001).
32. C.N. Jayarajah, A. Yekta, I. Manners, and M.A. Winnik, *Macromolecules*, **33**(**15**), 5693 (2000).
33. R. Ruffolo, C. Evans, X.H. Liu, Y. Ni, Z. Pang, P. Park, A. MacWilliams, X. Gu, X. Lu, A. Yekta, M.A. Winnik, and I. Manners, *Anal. Chem*., **72**, 1894 (2000).
34. O. Pekcan and S. Ugur, *J. Colloid Interface Sci*., **217**, 154 (1999).
35. O. Pekcan and S. Ugur, *Polymer*, **41**, 7531 (2000).
36. J.B. Birks, *Organic Molecular Photophysics*, Wiley-Interscience, New York (1975).
37. S.A. Rice, "Diffusion-Limited Reactions," in *Comprehensive Chemical Kinetics*,C.H. Bamford, C.F.H. Tipper, and R.G. Compton, Eds., Elsevier, Amsterdam (1985).
38. J. Crank, *The Mathematics of Diffusion*, Oxford University Press, London, 44 (1970).
39. D.Q. Vu, W.J. Koros, and S.J. Miller, *J. Membr. Sci*., **211**, 311 (2003).
40. H. Chen and D.S. Sholl, *J. Membr. Sci*., **269**, 152 (2006).
41. P.C. Ma, J.K. Kim, and B.Z. Tang, *Carbon*, **44**, 3232 (2006).
42. D.M. Delozier, K.A. Watson, J.G. Smith Jr., T.C. Clancy, and J.W. Connel, *Macromolecules*, **39**, 1731 (2006).
43. S. Ponomarev and M. Gouterman, in *The 6th Annual Pressure Sensitive Paint Workshop*, Settle, WA, Act. 6–8 (1998).
44. A.K. Kristi, J.N. Demas, B. Nguyen, A. Lockhart, W. Xu, and B.A. DeGraff, *Anal. Chem.,* **74**, 1111 (2002).